



Published in final edited form as:

Prostate. 2011 June 15; 71(9): 946–954. doi:10.1002/pros.21310.

PKC δ activation mediates angiogenesis *via* NADPH oxidase activity in PC-3 prostate cancer cells

Jeewon Kim¹, Tomoyoshi Koyanagi¹, and Daria Mochly-Rosen^{1,2}

¹Department of Chemical and Systems Biology, Stanford University, School of Medicine, Stanford, CA, 94305

Abstract

Background—PKC δ is generally known as a pro-apoptotic and anti-proliferative enzyme in human prostate cancer cells.

Methods—Here, we investigated the role of PKC δ on the growth of PC-3 human prostate cancer cells *in vivo* and *in vitro*.

Results—We found that sustained treatment with a specific PKC δ activator ($\psi\delta$ receptor for active C kinase, $\psi\delta$ RACK) increased growth of PC-3 xenografts. There was increased levels of HIF-1 α , vascular endothelial growth factor and CD31-positive cells in PC-3 xenografts, representative of increased tumor angiogenesis. Mechanistically, PKC δ activation increased the levels of reactive oxygen species (ROS) by binding to and phosphorylating NADPH oxidase, which induced its activity. Also, PKC δ -induced activation of NADPH oxidase increased the level of HIF-1 α .

Conclusions—Our results using tumors from the PC-3 xenograft model suggest that PKC δ activation increases angiogenic activity in androgen-independent PC-3 prostate cancer cells by increasing NADPH oxidase activity and HIF-1 α levels and thus may partly be responsible for increased angiogenesis in advanced prostate cancer.

Keywords

angiogenesis; HIF-1 α ; NADPH oxidase; prostate cancer; protein kinase C

Introduction

In the US, prostate cancer is the second leading cause of cancer-related deaths in males (1,2). The androgen-independent and advanced type of human prostate cancer cells, PC-3, shows higher levels of reactive oxygen species (ROS) as compared with the androgen-dependent and less invasive types (LNCap and DU 145) and inhibition of ROS generation reduces the invasiveness of the prostate cancer cell lines as shown by matrigel assay. More importantly, human prostate tumor tissues have elevated ROS levels and this was shown to correlate with increased levels of ROS-generating enzymes, like NADPH oxidase (3).

ROS are generated from a number of sources including NADPH oxidase, the mitochondrial electron transport system, xanthine oxidase, cytochrome p-450, and uncoupled nitric oxide synthase (4,5). Among these, the family of NADPH oxidase and the mitochondria systems have emerged as major sources of ROS production (6,7). NADPH oxidase is a major extra-

²Address for all correspondence: Daria Mochly-Rosen, Department of Chemical and Systems Biology, Stanford University, School of Medicine, Stanford, CA, 94305-5174, Tel: 650-725-7720, Fax: 650-723-4686, mochly@stanford.edu.

mitochondrial cellular source for producing ROS in a wide variety of non-phagocytic tissues and conditions, including inflammation against injurious stimulus, tissue fibrosis, atherosclerosis and several cancers including prostate cancer (8).

NADPH oxidase consists of membrane-bound subunits, gp91^{phox} and p22^{phox} which form the flavocytochrome b558 complex, together with the cytosolic subunits p40^{phox}, p47^{phox}, and p67^{phox}, as well as the small GTPase, Rac (4). Superoxide production is induced by assembly of these cytosolic and membrane-bound subunits, which is mediated through the phosphorylation of p47^{phox} (9). Because ROS mediates angiogenic signaling, NADPH oxidase is emerging as an important signaling mediator of angiogenesis, especially in cancer, and has been shown to increase in correlation with tumorigenic activity in various cancers (4). For example, Nox1, one of the homologues of the NADPH oxidase catalytic subunit gp91^{phox}, is highly expressed in human prostate cancer in correlation with increased hydrogen peroxide levels (10).

Phosphorylation of several serine residues of p47^{phox} subunit enables it to bind to membrane phospholipids and to interact with p22^{phox}, and brings the p67^{phox} subunit to the complex. The p67^{phox} binds and stabilizes an interaction of the complex with the small GTPase Rac, and the fully formed NADPH complex is able to generate superoxide radical (11,12). Therefore, phosphorylation of p47^{phox} is a critical step in the activation of NADPH oxidase. PKC isozymes are the major kinases responsible for inducing NADPH oxidase activation. PKC β II phosphorylates p47^{phox} and p67^{phox} cytosolic subunits in monocytes, inducing NADPH oxidase activity (12,13). PKC δ phosphorylates p67^{phox} in monocytes when treated with ZOP (an NADPH oxidase activator) (13). Also, p47^{phox} was found to be a substrate for PKC δ in human neutrophils (14) and PKC δ increased mRNA levels of the Nox1 present in vascular smooth muscle cells (15). However, the regulation of NADPH oxidase in the growth of PC-3 human prostate cancer in relation to angiogenesis has not been studied in detail *in vivo*.

Here, we determined the novel role of PKC δ and the mechanism involved in the growth of PC-3 tumor xenografts using PKC δ -selective peptide regulators. Our data from xenografts suggest that PKC δ can be a target in anti-cancer treatment for prostate cancer against angiogenesis in PC-3 human prostate tumors.

Materials and methods

Cell lines and cell culture

PC-3 human prostate cancer cells were obtained from the American Type Culture Collection (ATCC, Manassas, VA) and cultured in DMEM media with 10% fetal bovine serum (FBS, Gibco, NY) with 1% antibiotics (penicillin and streptomycin, Gibco, NY).

Materials

For Western blot analyses, rabbit antibodies directed against G α i-3 (C-10), anti-phospho threonine (9381), anti-phospho threonine-X-arginine (2351S) antibodies, anti-p47^{phox}(D-10) mouse monoclonal antibodies and PKC δ and ϵ antibodies were from Santa Cruz Biotechnology, Inc. (Santa Cruz, CA) and anti-GAPDH antibody (clone 6C5) was from Advanced Immunochemical (Long Beach, CA). HIF-1 α antibodies were from Bethyl Laboratories (Montgomery, TX).

Peptide synthesis and administration

The PKC δ -selective inhibitor (δ V1-1, amino acids 8-17 (SFNSYELGSL)) and activator (ψ δ RACK, amino acids 74-81 (MRAAEDPM)) were derived from the PKC δ V1 region and

synthesized by American Peptide Company and conjugated to a membrane-permeable TAT carrier peptide (residues 47-57, [YGRKKRRQRRR]) as previously described (16). TAT carrier peptide was used as a control. Peptides were delivered *in vivo* using Alzet osmotic mini-pumps (Alzet model 2001) as described (17). The peptides were dissolved in saline and administered at a constant rate (0.5 μ l/hr) corresponding to 2.4 or 24 mg/day/kg (3mM or 30mM of TAT), 1.4 mg/day/kg (1mM of δ V1-1) and 3.8 or 38 mg/day/kg (3mM or 30mM of ψ δ RACK). Pumps were replaced every 2 weeks because of the $t_{1/2}$ (about 2 weeks) of the peptides in the pump (17). Peptides were delivered for up to 4 weeks.

Xenograft tumor studies

Six week old male nude mice were purchased from Harlan (Indianapolis, IN) and housed at the animal care facility at Stanford University Medical Center (Stanford, CA). All mice were kept under standard temperature, humidity, and timed lighting conditions and provided mouse chow and water *ad libitum*. All animal experimentation was conducted in accordance with the Guide for Care and Use of Laboratory Animals prepared by the Institute of Laboratory Animal Resources, National Research Council, and published by the National Academy Press (revised 1996) and was approved by the Stanford University Animal Care and Use Committee. Five million PC-3 tumor cells were injected subcutaneously in the flank of male, 7-8 week old, athymic nude mice in a mixture of 1:1 serum-free medium and Matrigel (Beckton Dickinson, Bedford, MA). Peptide treatment began when the tumors reached a group average of 100mm³ after about 1 week. Tumor volume (mm³) was calculated using the equation $0.52 \times (\text{width (cm)}^2 \times \text{length (18)})$.

Immunofluorescence microscopy

Immunofluorescence was performed on fresh-frozen PC-3 tumor sections fixed in O.T.C. compound (Torrance, CA) using FITC-linked anti-mouse CD31 antibodies (1:50, BD Pharmingen, San Diego, CA).

Western blot analysis

Protein concentrations were determined using the Bradford assay. Ten micrograms of protein from tumors were resuspended in Laemmli buffer, loaded on SDS-PAGE and transferred onto nitrocellulose membranes. Membranes were probed with the indicated antibody followed by visualization with ECL.

Preparation of total cell lysates and fractionation

Samples were prepared as previously described (19,20).

Immunoprecipitation

Proteins (300-500 μ g) were solubilized in lysis buffer and the whole cell lysate was incubated with primary antibody against p47^{phox} overnight at 4 °C. Then the samples were precipitated with protein-A/G sepharose (Santa Cruz Biotech) at 4 °C for 1 hour and the immunoprecipitates were washed twice in HEPES buffer as previously described (20). The proteins in the immunoprecipitates were separated using SDS-PAGE and analyzed using immunoblotting.

NADPH oxidase activity assay

Cells were serum starved for 14 to 48 hours prior to the measurement and stimulated with 1% fetal bovine serum and/or chemicals as indicated. After washing twice with 1x PBS, cells were collected with 1x PBS containing protease inhibitor cocktail and phosphatase inhibitor cocktail I and II (Sigma, St. Louis, MO) using a cell scraper. The lysate was further homogenized using syringes with 25G needles. Measurement was performed by adding 10 μ l

of lysate into 200 μ l of reaction buffer (20 mM Tris-HCl pH 7.5, 150 mM NaCl, 1 mM EDTA, 1mM EGTA, 5 μ M lucigenin and 100 μ M NADPH). Chemiluminescence derived from superoxide and lucigenin were detected by a luminometer within 30 minutes after the addition of reaction buffer (Veritas, Turner Biosystems, Sunnyvale, CA).

RNA interference

Small interfering RNA (siRNA) duplexes targeting PKC δ were obtained from Santa Cruz Biotech (human, sc-36253, Santa Cruz, CA). PC-3 cells at ~60% confluency were transfected with control siRNA and PKC δ siRNA using transfection reagents from Gene Silencer (San Diego, CA) according to the manufacturer's instructions. The cells were collected 48 hours after transfection.

Measurement of vascular endothelial growth factor (VEGF) levels in serum

The concentration of VEGF in the serum was measured using an ELISA kit (human and mouse VEGF immunoassay, Quantikine, R&D Systems, Minneapolis, MN) according to the manufacturer's instructions.

Statistical analysis

Data are expressed as mean \pm SE. Unpaired Student's *t* test for differences between two groups, repeated ANOVA for differences over time and 1-factor ANOVA for differences among >2 groups were used to assess significance ($p < 0.05$).

Results

Figure 1. PKC δ activation increases PC-3 prostate tumor growth

PKC δ activation has been implicated in the growth of several epithelial cancers including prostate, breast and ovarian cancers (21-23). Here, we first compared the cellular distribution of PKC δ as a measure of its active level in PC-3 cells with that in a primary culture of normal human prostate epithelial cells (hPEC) [Figure 1A, left; cytosolic (C) fraction enzyme represents inactive PKC and particulate fraction enzyme (P) represents active PKC (20,24)]. PKC δ was more active in the PC-3 cells relative to the primary hPEC as evidenced by higher levels of this isozyme in the particulate fraction relative to the cytosolic fraction (Figure 1A, $n=3$ each). Also, PKC δ translocation increased by about 5 fold during the growth of PC-3 human prostate cancer cells in a xenograft model, *in vivo* (from 10% to 53%; Figure 1B, $p < 0.05$ vs. week 3). We have recently shown that the volume of PC-3 tumor xenografts increases significantly between week 3 and 5 and that angiogenesis in the tumor increased during that period [as measured by endothelial cell proliferation (20)]. The finding that PKC δ translocation increased significantly between week 3 and 4 and was maintained at similar levels afterwards suggests that PKC δ activation may be involved in angiogenesis and the growth of PC-3 tumors.

To examine the role of PKC δ in PC-3 xenograft tumor growth *in vivo*, PC-3 cancer cells were injected subcutaneously (5×10^6 cells) into the flank area of male nude mice. After 1 week, mice were treated with control peptide [TAT₄₇₋₅₇ cell-permeable carrier peptide] at 30mM (24 mg/kg/day), a PKC δ -selective inhibitor peptide coupled to TAT₄₇₋₅₇; δ V1-1 at 1mM (1.4 mg/kg/day) or a PKC δ -selective activator peptide coupled to TAT₄₇₋₅₇; ψ δ RACK (16) at 3mM or 30mM (3.8 or 38 mg/kg/day) for the following 4 weeks using Alzet osmotic pumps for sustained infusion (Figure 1C). Final tumor volume was 23% lower in the δ V1-1-treated group (440 ± 40 and 340 ± 80 , control vs. δ V1-1-treated group, $n=5-10$ each) and 50% higher in the 3mM ψ δ RACK-treated group (440 ± 40 and 660 ± 60 , control vs. ψ δ RACK-treated group, Figure 1C, *, $p < 0.05$, $n=5-6$ each, a 2-tailed Student's *t* test). The higher concentration of ψ δ RACK increased final tumor volume by 220% in the

$\psi\delta$ RACK-treated group (440 ± 40 and $1,280\pm 340$, TAT vs. $\psi\delta$ RACK-treated group, Figure 1C, *, $p<0.05$, $n=5-8$ each, Student's t test and repeated ANOVA). Final tumor volumes are shown in the insert (Figure 1C). These data suggest that PKC δ activation increases during the angiogenically active period of PC-3 tumor growth and that PKC δ activation increases tumor growth rate.

Figure 2. PKC δ activation increases tumor angiogenesis

We first observed that there were significantly higher CD31-positive tumor vessels in the $\psi\delta$ RACK-treated (30mM, 38 mg/kg/day) tumors compared to TAT controls (1600 ± 220 vs. 86 ± 3 %, $p<0.05$, Figure 2A and a graph). $\psi\delta$ RACK treatment did not induce apoptosis in this model as measured by TUNEL staining (data not shown). Based on these results, we focused our study on determining the role of PKC δ and angiogenic events during tumor growth.

We also observed increased HIF-1 α protein levels in the $\psi\delta$ RACK-treated tumors compared to the controls. At week 5, after 4 weeks of sustained treatment with $\psi\delta$ RACK (38 mg/kg/day), HIF-1 α levels increased by more than 3-fold as compared with the control (TAT-treated) group (Figure 2B, 0.15 ± 0.01 and 0.63 ± 0.70 , TAT vs $\psi\delta$ RACK, *, $p<0.05$, $n=3$ each). Of all the pro-angiogenic factors induced by HIF1- α , VEGF is particularly noteworthy, because it has potent angiogenic properties and is expressed in a large number of human cancers including prostate tumors (25). With $\psi\delta$ RACK treatment (38 mg/kg/day, 30mM), the human VEGF concentration in the serum increased by ~6-fold as compared with the control mice (Figure 2C, left, *, $p<0.05$, 330 ± 110 vs. $2,700\pm 920$ pg/ml/tumor weight, TAT vs. $\psi\delta$ RACK; $n=4$). However, there was no difference in the concentration of mouse VEGF between the two treatments (Figure 2C right, 190 ± 70 vs. 280 ± 100 pg/ml/tumor weight, TAT vs. $\psi\delta$ RACK) [VEGF concentration was normalized against tumor weight]. These data indicate that PKC δ activation promotes angiogenesis by increasing HIF1- α and pro-angiogenic growth factor VEGF levels in the human prostate cancer xenograft. Increased VEGF production was from human tumor cells and not from the mouse endothelial cells.

Figure 3. PKC δ regulates NADPH oxidase activity in PC-3 cells

ROS, which is found in a large number of tumors, has been reported to mediate angiogenic signaling by stimulating endothelial cell growth and migration (4). NADPH oxidase is one of the major cellular sources for continuously producing ROS intracellularly at low levels in a wide variety of cells (8). ROS production by NADPH oxidase can also be further activated by various growth factors and other stimuli (4). Furthermore, NADPH oxidase was shown to be more active in more aggressive prostate cancer cell lines (3). Based on these results, we examined the molecular mechanisms of increased angiogenesis with PKC δ activation by measuring NADPH oxidase activity in tumors treated with TAT or $\psi\delta$ RACK (Figure 3A). We used tumors obtained by the same protocol as described in Figure 1C, treated with TAT or $\psi\delta$ RACK (30mM). Lucigenin and superoxide-derived chemiluminescence was used as a measure of NADPH oxidase activity in the tissue lysates. $\psi\delta$ RACK treatment resulted in an ~80% increase in the catalytic activity of NADPH oxidase (Figure 3A) relative to TAT treatment.

Next, we observed the regulation of NADPH oxidase activity by PKC δ *in vitro*, using both the PKC δ isozyme-specific inhibitor and activator peptides in PC-3 cells (Figure 3B). Cells were serum starved and incubated with the PKC δ inhibitory peptide (δ V1-1; 1μ M) or the PKC δ activator peptide ($\psi\delta$ RACK; 1μ M). Treatment with the PKC δ -selective inhibitor decreased NADPH oxidase activity by more than 30% (125 ± 11 % and 97 ± 4 %, PMA vs. δ V1-1+PMA, *, $p<0.05$, Figure 3B, left panels). Activation of PKC δ with $\psi\delta$ RACK

increased NADPH oxidase activity by 22% ($100\pm 7\%$ and $122\pm 5\%$, 1% serum vs. $\psi\delta$ RACK +1% serum, *, $p<0.05$, Figure 3B, right panels). The difference between *in vivo* and *in vitro* data in NADPH oxidase activity with $\psi\delta$ RACK treatment may result from amplified induction of ROS from chronic hypoxia in solid tumors and the contribution of growth factors that may have stimulated PKC δ activity further *in vivo*. To confirm PKC δ regulation of NADPH oxidase activity, we knocked down the level of PKC δ using siRNA and assayed for the NADPH oxidase activity. Knock down using siRNA decreased the level of PKC δ by ~40% (Figure 3C, *, $p<0.05$, $n=3$ each) and decreased NADPH oxidase activity by more than 3 fold (Figure 3D, 6.0 ± 0.2 and 2.0 ± 0.1 , control vs. siRNA treated, *, $p<0.05$, $n=3$ each). These data show that PKC δ regulates NADPH oxidase activity *in vivo* and *in vitro* in PC-3 cancer cells.

Figure 4. PKC δ regulates NADPH oxidase by phosphorylating and inducing the translocation of NADPH oxidase subunit p47^{phox} to the membrane fraction

We then determined the molecular basis for activation of NADPH oxidase by PKC δ . As mentioned previously, PKC isozymes are the major kinases responsible for inducing NADPH oxidase activation (12,13). Because superoxide production is induced by assembly of the cytosolic and membrane-bound subunits of NADPH oxidase, a process triggered by the phosphorylation of p47^{phox} (12), we hypothesized that PKC δ phosphorylation of p47^{phox} may play a role in the regulation of NADPH oxidase activity in PC-3 cells. Treatment with $\psi\delta$ RACK for 4 weeks (30mM) significantly increased serine/threonine phosphorylation of a ~50kDa band by Western blot analysis of total tumor lysates. The level of the phosphorylated form of putative p47^{phox} was increased by ~5 fold with $\psi\delta$ RACK treatment compared to TAT controls (1.0 ± 0.2 and 5 ± 1 , TAT vs. $\psi\delta$ RACK, *, $p<0.05$, $n=3$ each, Figure 4A). When tumor lysates were immunoprecipitated (IP) with antibodies against p47^{phox}, the amount of co-immunoprecipitated PKC δ increased by ~150% after $\psi\delta$ RACK treatment as compared with TAT controls (Figure 4B). p47^{phox} was used as a loading control. We next set out to determine the phosphorylation levels of the co-immunoprecipitated p47^{phox} in the tumors. Immunoprecipitated p47^{phox} using anti-p47^{phox} antibodies was probed with anti-serine/threonine antibodies. With $\psi\delta$ RACK treatment, phosphorylation of the immunoprecipitated p47^{phox} increased by 6-fold as normalized by PKC δ (1.0 ± 0.4 and 6.0 ± 1.4 , TAT vs. $\psi\delta$ RACK, *, $p<0.05$, $n=3$, Figure 4C). Finally, the translocation of p47^{phox} from the cytosolic to the membrane (particulate) fraction increased significantly with $\psi\delta$ RACK treatment (1.0 ± 0.1 and 4.0 ± 0.9 , *, $p<0.05$, $n=3$, Figure 4D). These data suggest that $\psi\delta$ RACK-induced interaction of NADPH oxidase with PKC δ and phosphorylation of an NADPH oxidase subunit p47^{phox} and induction of its translocation to the cell membrane may partly explain the molecular basis for activation of NADPH oxidase by PKC δ .

Figure 5. PKC δ regulates HIF-1 α levels in PC-3 cells via NADPH oxidase

ROS produced in response to repeated cycles of hypoxia and normoxia was shown to induce angiogenic response by increasing HIF-1 α accumulation, which was regulated by NADPH oxidase in PC12 cells (5). Based on this and our data that PKC δ regulates NADPH oxidase activity (Figures 3) and PKC δ activation increased HIF-1 α levels (Figure 2), we hypothesized that PKC δ may regulate HIF-1 α levels through NADPH oxidase activity. PC-3 cells were serum starved for 14 hours and incubated with apocynin (a chemical inhibitor of NADPH oxidase, 1mM) for 5 minutes. Apocynin decreased HIF-1 α levels by more than 4-fold in the presence of 1% serum (Figure 5A, middle panel, $n=3$ each, *, $p<0.05$), showing that NADPH oxidase regulates HIF-1 α levels in PC-3 cells. Next, we found that PKC δ inhibition decreased HIF-1 α levels by almost 50% (1.0 ± 0.03 and $0.6\pm 0.12\%$, TAT vs. δ V1-1, $n=3$, Figure 5A, second to right panel). On the other hand, PKC δ activation increased HIF-1 α levels by more than 3-fold ($1.0\pm 0.03\%$ and $3.2\pm 0.5\%$,

TAT vs. $\psi\delta$ RACK, n=3-4, Figure 5A, far right panel). HIF-1 α levels were unchanged with δ V1-1 or $\psi\delta$ RACK in the presence of apocynin treatment (data not shown). These data suggest that PKC δ regulates HIF-1 α levels through NADPH oxidase.

A schematic diagram (Figure 5B) summarizes the regulation of tumor-induced angiogenesis *via* HIF-1 α levels through PKC δ and NADPH oxidase in PC-3 prostate cancer cells. Activated PKC δ can then phosphorylate substrates nearby. PKC δ activation increases phosphorylation of the p47^{phox} subunit of NADPH oxidase, which induces its translocation to the membrane and NADPH oxidase activation. Activated NADPH oxidase then produces large quantities of ROS, increases HIF-1 α levels and VEGF production from tumor cells, thus increasing angiogenic activity in tumors.

Conclusions

Identifying the role of specific PKC isozymes in tumors has been hampered by lack of isozyme-specific regulators for each PKC isozyme. Here, using an isozyme-selective inhibitor and an activator peptide for PKC δ (26-28), we show a novel role of PKC δ as an upstream regulator of NADPH oxidase activation leading to increased HIF-1 α levels, angiogenesis and tumor growth in PC-3 human prostate cancer. NADPH oxidase activation has been shown to mediate expression of HIF-1 α and VEGF and increase tumor growth in ovarian cancer (29). Also, in ~70% of prostate cancer patients, mRNA of catalytic subunit of NADPH oxidase, Nox1, was found only in tumor tissues but not in normal epithelium (10). These upregulated pro-survival signaling pathways in angiogenesis may contribute to the development of resistance to therapy in advanced prostate cancer patients. Development of a safe and targeted molecule to inhibit PKC δ may aid in reducing the resistance experienced by prostate cancer patients.

Previously, LNCaP human prostate cancer cells were shown to undergo apoptosis in response to phorbol esters (30). It was found that the apoptosis induced by phorbol 12-myristate 13-acetate in LNCaP cells was mediated by PKC δ (31). PKC δ was also shown to mediate prostate cancer cell apoptosis induced by chemotherapeutic agents (32). Therefore, PKC δ has been known to be a critical mediator of apoptosis induced by phorbol esters or anticancer drugs. As such, PKC δ was generally found to be pro-apoptotic (21,27,33). However, PKC δ was also reported to be the major kinase that promotes cell survival in mammary and ovarian cancer cells (22,23). Here we revealed a novel role of PKC δ in inducing angiogenesis and growth of PC-3 tumors.

Reactive oxygen species (ROS) mediate angiogenic signaling and NADPH oxidase is one of the major sources of ROS in endothelial cells (4). Increased NADPH oxidase activities correlate with tumorigenic activity in various cancers (8,10). Further, Nox1, a catalytic subunit of NADPH oxidase, was shown to play a critical role in tumor-induced angiogenesis. Inhibition of Nox1 by siRNA or diphenylene iodonium (DPI) inhibited synthesis of VEGF mRNA and protein in K-Ras transformed normal rat kidney cells. Mechanistically, Nox1 inhibition decreased ERK-dependent phosphorylation of Sp1 transcriptional factor and its binding to VEGF promoter (34).

Here, we show that PKC δ co-immunoprecipitates with a subunit of NADPH oxidase critical for its activation and to induce NADPH oxidase activation and promote angiogenesis. These data suggest that disruption of PKC δ -NADPH oxidase inter-molecular protein interactions can negatively modulate tumor-induced angiogenesis. More importantly, PKC δ can be both pro-survival and pro-apoptotic depending on the cell type and binding molecules available as previously mentioned, development of regulators of PKC δ in cancer therapy needs to be approached with caution.

In conclusion, we showed that PKC δ activation can increase NADPH oxidase activity and HIF-1 α levels, leading to increased angiogenesis and tumor growth in PC-3 human prostate tumors. Therefore, PKC δ inhibition may provide a useful adjuvant treatment to the current therapy for patients with prostate cancer by inhibiting tumor-induced angiogenesis.

Supplementary Material

Refer to Web version on PubMed Central for supplementary material.

Acknowledgments

We thank members of the Mochly-Rosen lab for valuable comments, especially Dr. Alice Vallentin; Dr. Erinn Bruno Rankin at the Department of Radiation Oncology at Stanford Medical School for technical and valuable advice, Dr. Donna Peehl and Ms Rosalie Nolley at the Department of Urology at Stanford Medical School for providing human cells; Dr. Adrienne Gordon for critique on the manuscript. We also thank Ms Marlene Martin for valuable assistance. This study was supported in part by PHS Grant Number CA09151 awarded by the National Cancer Institute, DHHS to J Kim.

This study was supported in part by PHS Grant Number CA09151 awarded by the National Cancer Institute, DHHS to J Kim.

Daria Mochly-Rosen is the founder of KAI Pharmaceuticals, Inc. However, none of the work described in this study was based on or supported by the company.

References

1. Jemal A, Siegel R, Ward E, Hao Y, Xu J, Thun MJ. Cancer statistics, 2009. *CA Cancer J Clin.* 2009; 59(4):225–249. [PubMed: 19474385]
2. Mostaghel EA, Montgomery B, Nelson PS. Castration-resistant prostate cancer: targeting androgen metabolic pathways in recurrent disease. *Urol Oncol.* 2009; 27(3):251–257. [PubMed: 19414113]
3. Kumar B, Koul S, Khandrika L, Meacham RB, Koul HK. Oxidative stress is inherent in prostate cancer cells and is required for aggressive phenotype. *Cancer Res.* 2008; 68(6):1777–1785. [PubMed: 18339858]
4. Ushio-Fukai M, Nakamura Y. Reactive oxygen species and angiogenesis: NADPH oxidase as target for cancer therapy. *Cancer Lett.* 2008; 266(1):37–52. [PubMed: 18406051]
5. Yuan G, Nanduri J, Khan S, Semenza GL, Prabhakar NR. Induction of HIF-1 α expression by intermittent hypoxia: involvement of NADPH oxidase, Ca²⁺ signaling, prolyl hydroxylases, and mTOR. *J Cell Physiol.* 2008; 217(3):674–685. [PubMed: 18651560]
6. Korge P, Ping P, Weiss JN. Reactive oxygen species production in energized cardiac mitochondria during hypoxia/reoxygenation: modulation by nitric oxide. *Circ Res.* 2008; 103(8):873–880. [PubMed: 18776040]
7. Lambeth JD, Krause KH, Clark RA. NOX enzymes as novel targets for drug development. *Semin Immunopathol.* 2008; 30(3):339–363. [PubMed: 18509646]
8. Lambeth JD. Nox enzymes, ROS, and chronic disease: an example of antagonistic pleiotropy. *Free Radic Biol Med.* 2007; 43(3):332–347. [PubMed: 17602948]
9. Bokoch GM, Knaus UG. NADPH oxidases: not just for leukocytes anymore! *Trends Biochem Sci.* 2003; 28(9):502–508. [PubMed: 13678962]
10. Lim SD, Sun C, Lambeth JD, Marshall F, Amin M, Chung L, Petros JA, Arnold RS. Increased Nox1 and hydrogen peroxide in prostate cancer. *Prostate.* 2005; 62(2):200–207. [PubMed: 15389790]
11. Kim YS, Morgan MJ, Choksi S, Liu ZG. TNF-induced activation of the Nox1 NADPH oxidase and its role in the induction of necrotic cell death. *Mol Cell.* 2007; 26(5):675–687. [PubMed: 17560373]
12. Siow YL, Au-Yeung KK, Woo CW, O K. Homocysteine stimulates phosphorylation of NADPH oxidase p47phox and p67phox subunits in monocytes via protein kinase C β activation. *Biochem J.* 2006; 398(1):73–82. [PubMed: 16626305]

13. Zhao X, Xu B, Bhattacharjee A, Oldfield CM, Wientjes FB, Feldman GM, Cathcart MK. Protein kinase Cdelta regulates p67phox phosphorylation in human monocytes. *J Leukoc Biol.* 2005; 77(3):414–420. [PubMed: 15591124]
14. Remijsen QF, Fontayne A, Verdonck F, Clynen E, Schoofs L, Willems J. The antimicrobial peptide parabutoporin competes with p47(phox) as a PKC-substrate and inhibits NADPH oxidase in human neutrophils. *FEBS Lett.* 2006; 580(26):6206–6210. [PubMed: 17069809]
15. Fan CY, Katsuyama M, Yabe-Nishimura C. PKCdelta mediates up-regulation of NOX1, a catalytic subunit of NADPH oxidase, via transactivation of the EGF receptor: possible involvement of PKCdelta in vascular hypertrophy. *Biochem J.* 2005; 390(Pt 3):761–767. [PubMed: 15913451]
16. Chen L, Hahn H, Wu G, Chen CH, Liron T, Schechtman D, Cavallaro G, Banci L, Guo Y, Bolli R, Dorn GW 2nd, Mochly-Rosen D. Opposing cardioprotective actions and parallel hypertrophic effects of delta PKC and epsilon PKC. *Proc Natl Acad Sci U S A.* 2001; 98(20):11114–11119. [PubMed: 11553773]
17. Inagaki K, Begley R, Ikeno F, Mochly-Rosen D. Cardioprotection by epsilon-protein kinase C activation from ischemia: continuous delivery and antiarrhythmic effect of an epsilon-protein kinase C-activating peptide. *Circulation.* 2005; 111(1):44–50. [PubMed: 15611364]
18. McMullin RP, Mutton LN, Bieberich CJ. Hoxb13 regulatory elements mediate transgene expression during prostate organogenesis and carcinogenesis. *Dev Dyn.* 2009; 238(3):664–672. [PubMed: 19191217]
19. Begley R, Liron T, Baryza J, Mochly-Rosen D. Biodistribution of intracellularly acting peptides conjugated reversibly to Tat. *Biochem Biophys Res Commun.* 2004; 318(4):949–954. [PubMed: 15147964]
20. Kim J, Choi YL, Vallentin A, Hunrichs BS, Hellerstein MK, Peehl DM, Mochly-Rosen D. Centrosomal PKCbetaII and pericentrin are critical for human prostate cancer growth and angiogenesis. *Cancer Res.* 2008; 68(16):6831–6839. [PubMed: 18701509]
21. Griner EM, Kazanietz MG. Protein kinase C and other diacylglycerol effectors in cancer. *Nat Rev Cancer.* 2007; 7(4):281–294. [PubMed: 17384583]
22. Grossoni VC, Falbo KB, Kazanietz MG, de Kier Joffe ED, Urtreger AJ. Protein kinase C delta enhances proliferation and survival of murine mammary cells. *Mol Carcinog.* 2007; 46(5):381–390. [PubMed: 17219421]
23. Lee JW, Park JA, Kim SH, Seo JH, Lim KJ, Jeong JW, Jeong CH, Chun KH, Lee SK, Kwon YG, Kim KW. Protein kinase C-delta regulates the stability of hypoxia-inducible factor-1 alpha under hypoxia. *Cancer Sci.* 2007; 98(9):1476–1481. [PubMed: 17608772]
24. Kraft AS, Anderson WB, Cooper HL, Sando JJ. Decrease in cytosolic calcium/phospholipid-dependent protein kinase activity following phorbol ester treatment of EL4 thymoma cells. *J Biol Chem.* 1982; 257(22):13193–13196. [PubMed: 7142138]
25. Rankin EB, Giaccia AJ. The role of hypoxia-inducible factors in tumorigenesis. *Cell Death Differ.* 2008; 15(4):678–685. [PubMed: 18259193]
26. Bright R, Raval AP, Dembner JM, Perez-Pinzon MA, Steinberg GK, Yenari MA, Mochly-Rosen D. Protein kinase C delta mediates cerebral reperfusion injury in vivo. *J Neurosci.* 2004; 24(31):6880–6888. [PubMed: 15295022]
27. Murriel CL, Churchill E, Inagaki K, Szweda LI, Mochly-Rosen D. Protein kinase Cdelta activation induces apoptosis in response to cardiac ischemia and reperfusion damage: a mechanism involving BAD and the mitochondria. *J Biol Chem.* 2004; 279(46):47985–47991. [PubMed: 15339931]
28. Qi X, Mochly-Rosen D. The PKCdelta -Abl complex communicates ER stress to the mitochondria - an essential step in subsequent apoptosis. *J Cell Sci.* 2008; 121(Pt 6):804–813. [PubMed: 18285444]
29. Xia C, Meng Q, Liu LZ, Rojanasakul Y, Wang XR, Jiang BH. Reactive oxygen species regulate angiogenesis and tumor growth through vascular endothelial growth factor. *Cancer Res.* 2007; 67(22):10823–10830. [PubMed: 18006827]
30. Xiao L, Gonzalez-Guerrico A, Kazanietz MG. PKC-mediated secretion of death factors in LNCaP prostate cancer cells is regulated by androgens. *Mol Carcinog.* 2009; 48(3):187–195. [PubMed: 18756441]

31. Gavrielides MV, Gonzalez-Guerrico AM, Riobo NA, Kazanietz MG. Androgens regulate protein kinase Cdelta transcription and modulate its apoptotic function in prostate cancer cells. *Cancer Res.* 2006; 66(24):11792–11801. [PubMed: 17178875]
32. Sumitomo M, Ohba M, Asakuma J, Asano T, Kuroki T, Hayakawa M. Protein kinase Cdelta amplifies ceramide formation via mitochondrial signaling in prostate cancer cells. *J Clin Invest.* 2002; 109(6):827–836. [PubMed: 11901191]
33. Murriel CL, Mochly-Rosen D. Opposing roles of delta and epsilonPKC in cardiac ischemia and reperfusion: targeting the apoptotic machinery. *Arch Biochem Biophys.* 2003; 420(2):246–254. [PubMed: 14654063]
34. Komatsu D, Kato M, Nakayama J, Miyagawa S, Kamata T. NADPH oxidase 1 plays a critical mediating role in oncogenic Ras-induced vascular endothelial growth factor expression. *Oncogene.* 2008; 27(34):4724–4732. [PubMed: 18454179]
35. Steinberg SF. Distinctive activation mechanisms and functions for protein kinase Cdelta. *Biochem J.* 2004; 384(Pt 3):449–459. [PubMed: 15491280]
36. Talior I, Tennenbaum T, Kuroki T, Eldar-Finkelman H. PKC-delta-dependent activation of oxidative stress in adipocytes of obese and insulin-resistant mice: role for NADPH oxidase. *Am J Physiol Endocrinol Metab.* 2005; 288(2):E405–411. [PubMed: 15507533]

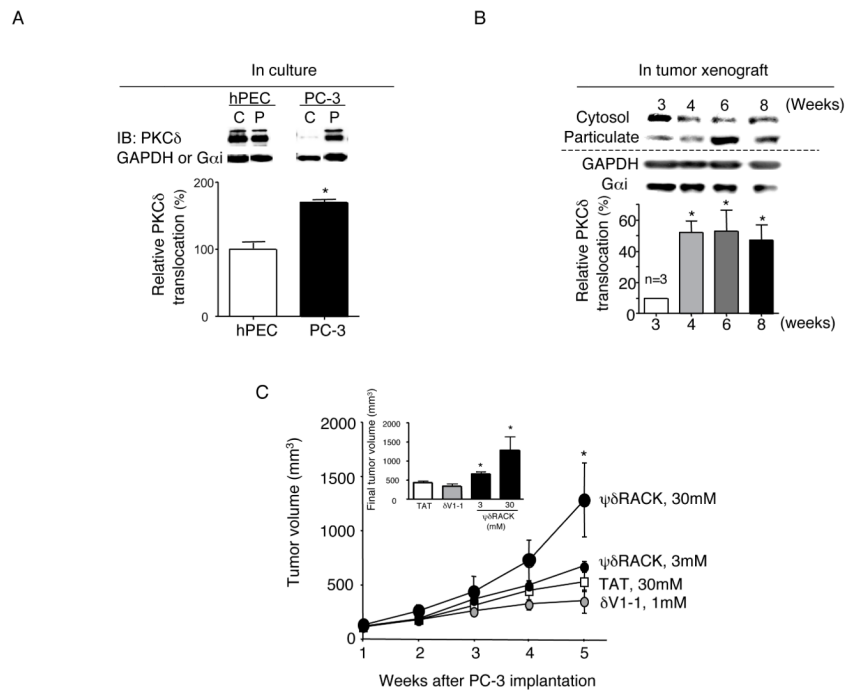


Fig. 1. PKC δ activation increases PC-3 prostate tumor growth

(A) The level of the active form of PKC δ was determined by Western blot analyses of cytosolic (C) and particulate (P) fractions from primary normal human prostate epithelial cells (hPEC) and PC-3 cells grown in culture. Cells were fractionated into cytosolic and particulate fractions as described in Methods. Quantification of the active forms of PKC δ (translocation; expressed as percentage of PKC isozyme in the particulate fraction over sum of cytosolic and particulate fraction enzymes, *i.e.*, total cellular enzyme) is provided in the graph below ($n=3$, *; $p<0.05$). A 2-tailed Student's *t* test was used to determine significance. Loading controls for cytosolic and particulate fractions (GAPDH and G α i) are shown in the lower bands. IB; immunoblot. (B) PC-3 xenografts were grown *s.c.* on nude mice for up to 8 weeks and tumors were obtained at weeks 3-8. PKC δ translocation was analyzed using Western blot and quantification is shown on the graph below ($n=3$, *; $p<0.05$) *vs.* week 3. (C) One week after PC-3 cell injection, mice were implanted with osmotic pumps with control peptide (TAT) at 24 mg/kg/day (30mM) or δ V1-1 conjugated to TAT at 1.4 mg/kg/day (1mM) or ψ δ RACK at 3.8 or 38 mg/kg/day (3mM or 30mM). The peptides were dissolved in saline and administered at a constant rate (0.5 μ l/hr) for 2 weeks and were replaced once for the next 2 weeks. Tumor volume was measured weekly. Tumors were excised and weighed at week 5. (White squares, TAT; small gray circles, δ V1-1; small black circles, 3mM ψ δ RACK and large black ovals, 30mM ψ δ RACK, *; $p<0.05$, repeated ANOVA, $n=5-8$ each, TAT *vs.* 30mM ψ δ RACK-treated group). An inserted graph shows final tumor volumes of each treatment group.

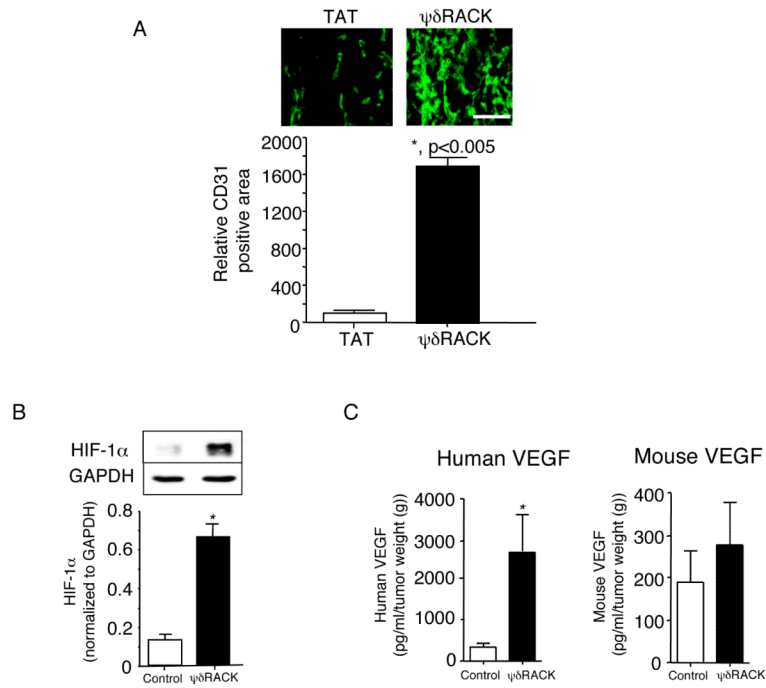


Fig. 2. PKCδ activation increases tumor angiogenesis

(A) The level of angiogenesis at the end of the 5-week growth was measured with immunofluorescence by staining blood vessels with anti-CD31 monoclonal antibodies conjugated with FITC (n=3 each, *, p<0.05, Scale bar: 10µm). (B) One week after PC-3 cell injection, mice were implanted with osmotic pumps with control peptide (TAT) or ψδRACK at 38 mg/kg/day (30mM) for 4 weeks. HIF-1α levels were measured by Western blot analyses using whole cell lysates from tumors (Figure 2B left, *, p<0.05 *t* test, n=3 each). GAPDH was used as a loading control. (C) Next, human VEGF concentration was measured in the serum from mice treated with control peptide (TAT) or ψδRACK by ELISA (Figure 2C left, *, p<0.05, n=4 each). Mouse VEGF concentration was measured in the serum from mice treated with control peptide (TAT) or ψδRACK by ELISA (Figure 2C, right).

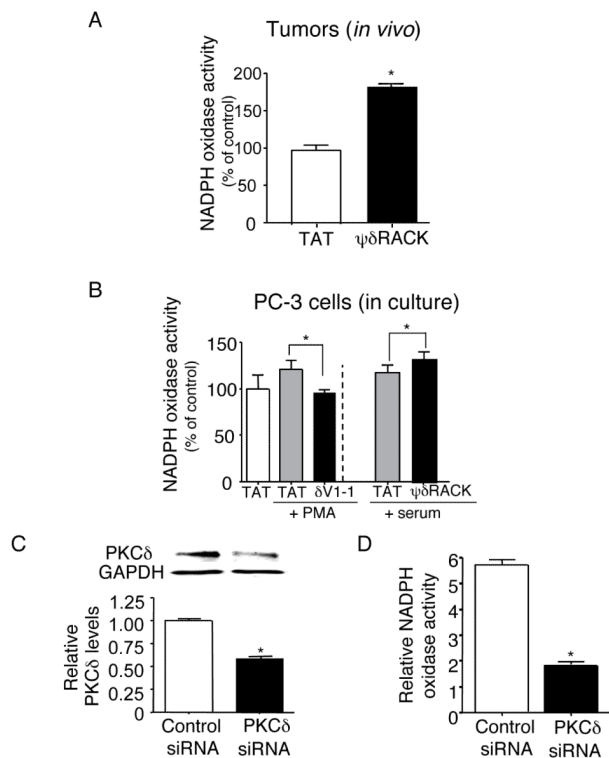


Fig. 3. PKC δ regulates NADPH oxidase activities in PC-3 cells

(A) Tumors as described in Figure 1C were analyzed for NADPH oxidase activity. Whole lysates of tumors in PBS with phosphatase and protease inhibitor cocktail were added with lucigenin. Chemiluminescence derived from superoxide and lucigenin was measured using a luminometer ($n=5$ each). A 2-tailed Student's t test was used to determine significance. (B) Cells were serum starved for 14 hours and first incubated with PKC δ inhibitor peptide ($\delta V1-1$, $1\mu M$) or PKC δ activator peptide ($\psi\delta RACK$, $1\mu M$) for 15 minutes. After incubation with $1nM$ PMA or serum for 30 minutes, whole cell lysate was used for the assay. A 2-tailed Student's t test was used to determine significance ($n=5-6$ for each treatment). (C) The levels of PKC δ in PC-3 cells were knocked down using siRNA. (D) To test PKC δ regulation of NADPH oxidase activity, NADPH oxidase activities were measured in the cells treated with control siRNA or siRNA of PKC δ . A 2-tailed Student's t test was used to determine significance ($n=3$ for each, *, $p<0.05$, t test).

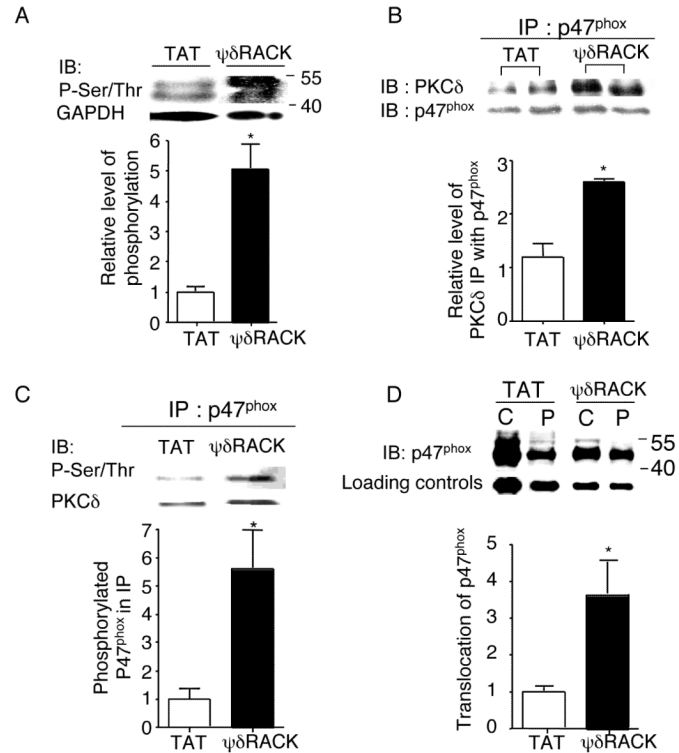


Fig. 4. PKC δ regulates NADPH oxidase activity by phosphorylating p47^{phox} and inducing its translocation to the membrane fraction

(A) Western blot analyses were performed with total cell lysates of PC-3 tumors treated with TAT or 38 mg/kg/day of $\psi\delta$ RACK for 4 weeks and immunoblotted with antibodies against phospho-serine/threonine (Ser/Thr) (*; $p < 0.05$, $n = 3$ each, Figure 4A). GAPDH was used as a loading control. (B) Tumor lysates were immunoprecipitated with antibodies against p47^{phox} and probed for PKC δ . (*; $p < 0.05$, $n = 3$ each, Figure 4B). p47^{phox} was used as a loading control. (C) Phosphorylation levels of the co-immunoprecipitated p47^{phox} were checked by probing with anti-Ser/Thr antibodies (*; $p < 0.05$, $n = 3$ each, Figure 4C). PKC δ was used as a loading control. (D) Finally, tumor lysates were fractionated (as described in the methods) and the translocation of p47^{phox} from the cytosolic to the membrane (particulate) fraction was determined by probing each fraction with anti-p47^{phox} antibodies (Figure 4D, *; $p < 0.05$, $n = 3$ each). GAPDH or Gai was used as a loading control (IB: immunoblot).

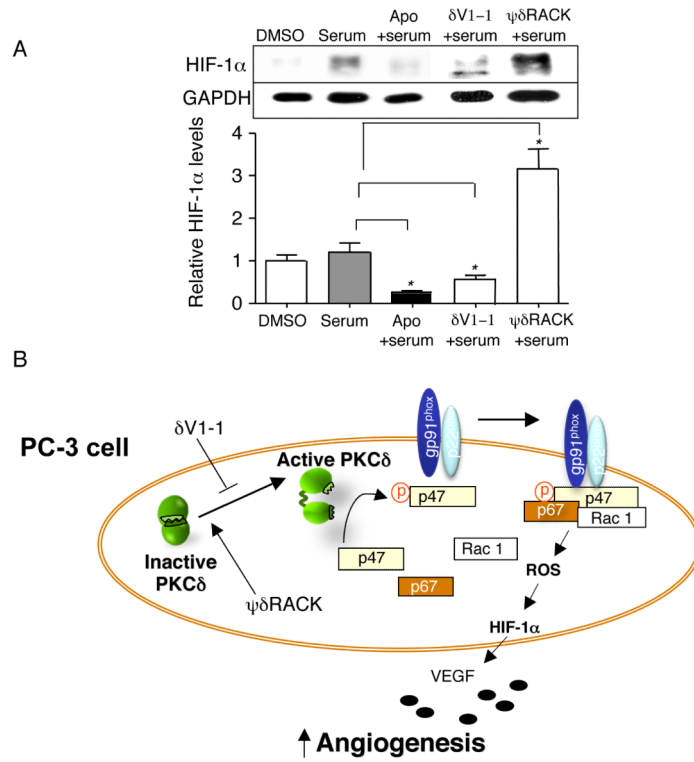


Fig. 5. PKCδ regulates HIF-1α levels in PC-3 cells via NADPH oxidase
 (A) PKCδ regulates HIF-1α levels via NADPH oxidase. PC-3 cells were serum starved for 14 hours and incubated with apocynin (an anti-oxidant and a chemical inhibitor of NADPH oxidase, 1mM) for 5 minutes in the presence of 1% serum (Figure 5A, n=3 each, *, p<0.05). Also, the PC-3 cells were treated with δV1-1 and ψδRACK at 1μM for 4 hours in the presence of 1% serum. The peptides were treated every 1.5 hours and the cells were lysed for Western blot analyses. (B) A schematic diagram summarizes the regulation of tumor-induced angiogenesis via HIF-1α levels by PKCδ and NADPH oxidase in PC-3 cancer cells. p47; p47^{phox} and p67; p67^{phox}.